A BIDIRECTIONAL PWM THREE-PHASE STEP-DOWN RECTIFIER BASED ON THE DIFFERENTIAL MODE POWER CONVERSION PRINCIPLE

Edward Fuentealba Vidal
Electric Engineering Department
University of Antofagasta
P.O.Box 170
Antofagasta – CHILE
efuentealba@ieee.org

Ivan Eidt Colling
Electrical Engineering Department
Federal University of Paraná
CEP 81531-990
Curitiba – PR – Brasil
ivan@eletrica.ufpr.br

Ivo Barbi
Power Electronics Institute
Federal University of Santa Catarina
P.O.Box 5119 – CEP 88040-970
Florianópolis – SC - BRAZIL
ivobarbi@inep.ufsc.br

Abstract – This paper presents a new three-phase rectifier that allows the operation as rectifier or inverter, with the use of three conventional switching cells. This reversion of power flow can be obtained simply by the inverting two reference currents. The system is analyzed as a connection of three independent lower order subsystems, controlled by sliding regime with decentralized switching scheme. The output voltage can be lower, equal or greater than the peak of the input voltage. The operation stages, equations, control strategy and design of the converter are presented. Finally, experimental results are shown for operation as inverter and rectifier.

Index Terms – ***AC-DC power conversion, DC-AC power conversion, power quality, power supplies, variable structure system***

I. INTRODUCTION

In the conventional three-phase PWM rectifier using the standard commutation cells shown in Fig. 1, the output DC voltage is greater than the peak value of the main voltage. In order to obtain lower output voltage, it is necessary to add another stage, as a bidirectional step-down DC-DC converter as shown in Fig. 1.

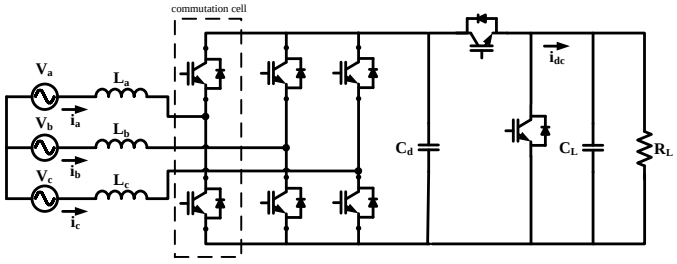

Fig. 1. Bidirectional PWM three-phase rectifier connected with to DC-DC converter.

It is possible to employ the classic step-down three-phase PWM rectifier, so that is not necessary to use another stage, as shown in Fig. 2. However, the converter does not employ the conventional commutation cell to operate properly. In this converter a diode is used in series with each switch. This contributes contribute to increase loss, cost, and complexity. Another disadvantage of this converter is that, if it is meant to perform DC-to-AC power transfer, the polarity of the voltage at the DC side must be inverted.

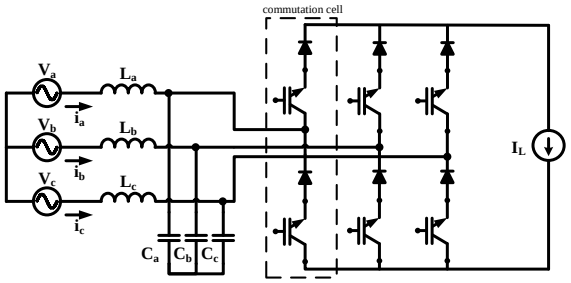

Fig. 2. Bidirectional step-down PWM three-phase rectifier.

These characteristics of the conventional converters shown in Fig. 1 and Fig. 2 indicate the necessity to find a different topology for three-phase rectification with nearly unity power factor, using conventional commutation cell and also capable to reduce the output DC voltage, without the addition of a second converter.

An alternative to single-phase case was presented by Colling and Barbi [1], [2], which by its turn was a development of the circuit proposed by Cáceres and Barbi [3], [4]. The topology is shown in Fig. 3, and has the following properties:

a) it is bidirectional;
b) the AC current, if controlled properly, is an image of the AC voltage, which allows to obtain unity power factor;
c) the DC output voltage is lower than the peak value of the AC input voltage;
d) it employs two conventional commutation cells.

The converter shown in Fig. 3 satisfied most of the design requirements. For this reason, in this paper, its three-phase version is presented.

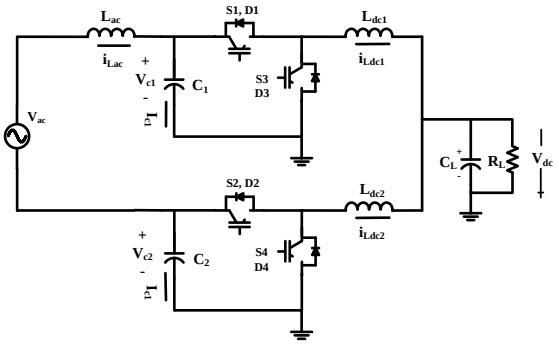

Fig. 3. Bidirectional high power factor step-down rectifier proposed by Colling and Barbi [1], [2].

II. OPERATION PRINCIPLE OF THE PROPOSED TOPOLOGY

The structure of Fig. 3 can be divided in two subconverters. The goal of the lower one (S2D2, S4D4, L_{dc2}, C_2) consists of keeping a sinusoidal voltage with a DC level on capacitor C_2. This DC level must be higher than V_{dc}. The upper subconverter (S1D1, S3D3, L_{dc1}, C_1, L_{ac}) controls the voltage on capacitor C_1, whose AC component must be complementary to that of V_{c2}. Besides that, it must adjust the value of the current i_{Lac} to obtain a high power factor [1], [2], [5].

The three-phase topology is shown in Fig. 4. It was presented by Colling and Barbi [6], with further developments in [7]. The converter used in phase C has the same function as the lower converter of Fig. 3. The converters used in the phases A and B adjust the values of the current i_{LacA} and i_{LacB}.

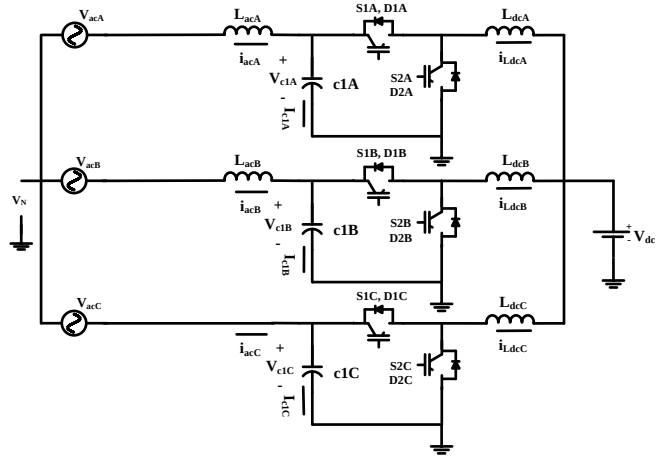

Fig. 4. New bidirectional step-down PWM three-phase rectifier.

The operation of the circuit demands a DC level on the capacitors c1A, c1B, and c1C in such a way that their voltages will never be inferior to V_{dc}. On the phase C capacitor, a DC level is imposed which is naturally established on the other two capacitors. This voltage is not perceived by the three-phase system, or by inductors L_{acA} and L_{acB}.

Phase C current is a dependent variable, since the neutral point of the three-phase system, is not connected to ground. For this reason, it is not necessary to have an inductor connected to phase C.

In order to begin the analysis of the topology, the three-phase circuit is separated into three lower-order interacting subsystems, each one associated to a phase of the power system.

Fig. 5a shows the subsystem associated to phase A, denominated converter A. It is of third order and its mission is to impose the current i_{acA}, no matter the value of (V_{acA}+V_N). Likewise, converter B (Fig. 5b) must control i_{acB}. Converter C (Fig. 5c) is a system of second order and must maintain voltage V_{c1C} close to its reference, regardless of the value of (i_{acA} + i_{acB}).

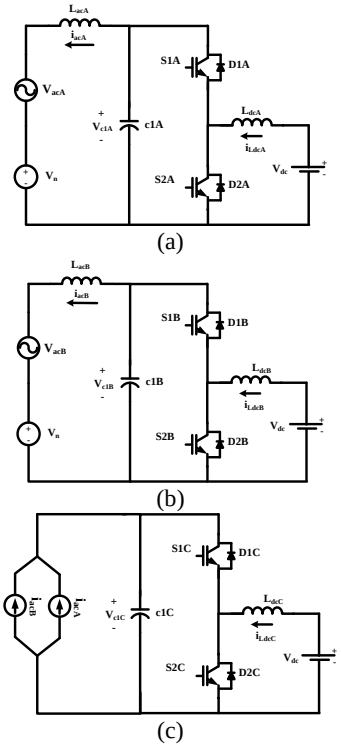

Fig. 5. The three-phase system is separated into three subsystems of lower order: (a) Converter associated to phase A, responsible by the imposition of i_{acA}. (b) Converter B, responsible by i_{acB}. (c) Converter C responsible for the control the voltage V_{c1C}.

A. Considerations for the operation of the converter C.

As stated before, converter C controls the voltage on C_{c1C} whose reference is a sinusoidal signal with a DC level that is given by eq.(1). Asterisks indicate reference values and ω represents the mains angular frequency.

$$V_{c1C}(t) = V^*_{c1Cdc} + V^*_{c1Cacp} \cdot \sin(\omega t + \phi_C) \quad (1)$$

The best distribution happens when voltage $V^*_{c1Cac}(t)$ is equal to the voltage of phase C. In this way, in steady state the three converters process the same power. Furthermore, V_N becomes constant, stabilizing about V^*_{c1Cdc}, the other voltages adapt themselves with proper magnitudes and phase. The duty cycle of converter C is given by eq.(2).

$$d_C(t) = 1 - \frac{V_{dc}}{V^*_{c1Cdc} + V^*_{c1Cacp} \cdot \sin(\omega t + \phi_C)} \quad (2)$$

To simplify the analysis the semiconductors are replaced by ideal switches. The switches S1C and S2C receive complementary pulses to prevent the discontinuous conduction mode in the L_{dcC} inductor. So, in the diagram shown in Fig. 6, only two structures are allowed: the first operating stage is defined when S2C - D2C is turned on and S1C - D1C is off $(\gamma = 1)$; the second one, represented by $(\gamma = 0)$, occurs when S1C - D1C is turned on and S2C - D2C is off.

Defining $\bar{\gamma} = 1 - \gamma$ and grouping the equations of the two operating stages in a matrix and defining the error of state

variables as $\varepsilon_{vc1C} = v_{vc1C} - v^*_{vc1C}$ and $\varepsilon_{iLdcC} = i_{iLdcC} - i^*_{iLdcC}$, where ε_{vc1C} is the feedback voltage error to v_{c1C} and ε_{idcC} is the feedback current error to i_{LdcC}, it is possible to obtain eq.(3).

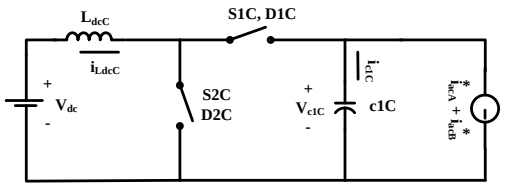

Fig. 6. Simplified structure of converter C.

$$\begin{bmatrix} \frac{d\varepsilon_{vc1C}}{dt} \\ \frac{d\varepsilon_{iLdcC}}{dt} \end{bmatrix} = \begin{bmatrix} i_{LdcC}/C_{1C} \\ -v_{c1C}/L_{dcC} \end{bmatrix} \cdot \bar{\gamma} + \begin{bmatrix} \left(i^*_{acA} + i^*_{acB}\right)/C_{1C} \\ V_{dc}/L_{dcC} \end{bmatrix} - \frac{d}{dt}\begin{bmatrix} v^*_{c1C} \\ i^*_{LdcC} \end{bmatrix} \quad (3)$$

The term $\frac{d}{dt}\left[v^*_{c1C} \quad i^*_{LdcC}\right]^T$ can be omitted in eq.(3) because the main frequency of V_{c1C} is ω and the main frequencies of current i_{LdcC} are ω and 2ω shown in eq.(7).. They are considered stationary compared to switching frequencies.

B. Considerations for the operation of converters A and B

Since converter A and B have the same operational stages. They only differ in regard to the reference current signals.

The output variable of converter A is the current i_{acA}, whose function of reference is given by eq.(4). For the operation as rectifier, π rad are added to the argument of the sine function. Voltage V_{c1A} is shaped so as to allow the current to follow its reference of i^*_{acA}.

$$i^*_{acA}(t) = I^*_{acA} \cdot \sin(\omega t + \phi_A) \quad (4)$$

V_{c1C} in steady state is such that the voltage V_N practically remains constant in the established DC level. Voltage V_{c1A} is shaped so as to allow the current to follow its reference i^*_{acA}. Besides that, in steady state, V_N remains practically constant at the established DC level, the voltage of the two other capacitors are given approximately by eq.(5) and eq.(6).

$$V_{c1A}(t) = V^*_{c1Cdc} + V_{acA} \quad (5)$$

$$V_{c1B}(t) = V^*_{c1Cdc} + V_{acB} \quad (6)$$

Considering the energy balance, an expression for the DC current in L_{dcA} can be obtained:

$$\begin{aligned} P_{dc} &= P_{ac} \\ V_{dc} \cdot i_{LdcC} &= V_{c1C} \cdot \left(i_{acC} + i_{Lc1C}\right) \end{aligned} \quad (7)$$

$$i_{LdcC}(t) = \frac{V^*_{c1Cdc} \cdot I^*_{acp} \cdot sen(\omega t + \phi_A)}{V_{dc}} + \frac{I^*_{acp} \cdot V_{c1Cacp}}{2 \cdot V_{dc}} \cdot \left(1 - \cos\left(2(\omega t + \phi_A)\right)\right) + \omega \cdot C_{c1C} \left\{ \frac{V^*_{c1Cdc} \cdot V_{c1Cacp} \cdot \cos(\omega t + \phi_A)}{V_{dc}} + \left\{ \frac{V^2_{c1Cacp}}{2 \cdot V_{dc}} \cdot sen\left(2(\omega t + \phi_A)\right) \right\} \right\} \quad (8)$$

The structure that represents converter A is shown in Fig. 7. An analysis similar to that of converter C is applied here considering the errors as: $\varepsilon_{iacA} = i_{iacA} - i^*_{iacA}$, $\varepsilon_{vc1A} = v_{vc1A} - v^*_{vc1A}$ and $\varepsilon_{iLdcA} = i_{iLdcA} - i^*_{iLdcA}$. Equation (9) is the resulting state equation for this structure.

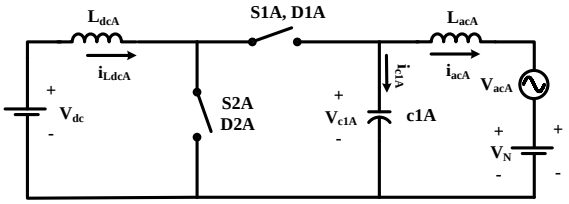

Fig. 7. Simplified structure of converter A [1], [2], and [6].

$$\begin{bmatrix} \frac{d\varepsilon_{iacA}}{dt} \\ \frac{d\varepsilon_{vc1A}}{dt} \\ \frac{d\varepsilon_{iLdcA}}{dt} \end{bmatrix} = \begin{bmatrix} V_{c1A}/L_{acA} \\ -i_{acA}/c1A \\ 0 \end{bmatrix} + \begin{bmatrix} 0 \\ i_{LdcA}/c1A \\ -V_{c1A}/L_{dcA} \end{bmatrix} \cdot \bar{\gamma} - \begin{bmatrix} -\left(V_{acA} + V_N\right)/L_{acA} \\ 0 \\ V_{dc}/L_{dcA} \end{bmatrix} \quad (9)$$

Fig. 8 shows the main voltage and current waveforms of the system in steady state, without considering switching frequencies. The mains voltages are shown in the top of Fig. 8, in the middle are shown voltages on c1A, c1B and c1C. The DC inductor currents are shown at the bottom of the Fig. 8.

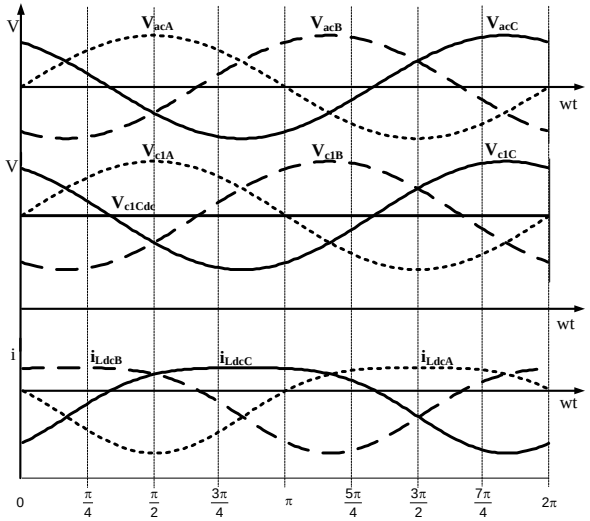

Fig. 8. Main steady-state waveforms of three-phase step-down rectifier.

III. CONTROL STRATEGY

For the original, single-phase step-up inverter proposed by Cáceres and Barbi [3], [4], different techniques have been tested and proposed: application of pulse-width modulation using the model of "PWM" switch to obtain the small-signal transfer function, feed-forward control and sliding mode or sliding regime.

From these mentioned solutions in [3] and [4] the last one showed the best characteristics of stability and robustness to the system. Based on this result the sliding regime with decentralized switching scheme is chosen. In this scheme, the whole system is considered as the interconnection of two or more subsystems, each one driven by an independent single-input control circuit. In each subconverter, one of the variables is the ruling parameter, and for this one a reference is defined. The other ones are “secondary variables”, whose

errors are obtained through high-pass filters [2], [6], [8], [9] and [10]. In this way, converter A has i_{acA} as ruling parameter and i_{LdcA} and V_{c1A} as secondary variables. The converter B has i_{acB} as ruling parameter, and i_{LdcB} and V_{c1B} as secondary variables. Finally, the ruling parameter of converter C is V_{c1C}, while i_{LdcC} is its secondary variable [6]. Deeper explanations concerning the control technique can be found in the aforementioned references, as well as in [5], [12], [13] and [14].

Thus, converters A and B are responsible for i_{acA} and i_{acB}, respectively. In phase C, circulates the inverted sum of this two currents, therefore the current i_{acC} is controlled indirectly. Three sliding surfaces are defined, one for each converter, given by equations (10), (11) and (12).

$$\sigma_A = S_3 \cdot \varepsilon_{iacA} + S_4 \cdot \varepsilon_{Vc1A} + S_5 \cdot \varepsilon_{iLdcA} \quad (10)$$

$$\sigma_B = S_6 \cdot \varepsilon_{iacB} + S_7 \cdot \varepsilon_{Vc1B} + S_8 \cdot \varepsilon_{iLdcB} \quad (11)$$

$$\sigma_C = S_1 \cdot \varepsilon_{Vc1C} + S_2 \cdot \varepsilon_{iLdcC} \quad (12)$$

The whole system is of eighth order (without counting the influence of the high-pass filters), but with the decentralized switching scheme, a controller is assigned to a cell, independently of the other cells.

The exposed circuit does not present restrictions to the relative values of voltages (DC and AC): DC level can be lower, equal or higher than the AC main peak voltage. In addition, this circuit is able to work as rectifier or inverter, only with the direction change of the two currents of references (i^*_{acA} and i^*_{acB}).

The election of the S_i parameters must be done satisfying some restrictions [1], [2] and [6]. For the sake of simplicity only the restrictions for converter C are presented; the relations for converters A and B are similar.

The ratio between S_1 and S_2 must be limited according to eq.(13), with $Z_{nC} = \sqrt{L_{dcC}/c1C}$. V_{c1C} by its turn, is limited by the equation (14), so that the system does not escape from the sliding surface. The switching frequency as a function of time is presented by eq.(15).

$$0 < \frac{S_1}{S_2} < \frac{V_{dc}}{Z_{nC}^{\,2} \cdot \left(I^*_{acA} + I^*_{acB}\right)} \quad (13)$$

$$V_{c1C} > V_{dc} + \max\left\{\frac{S_1}{S_2} \cdot Z_{nC}^2 \cdot \left[i^*_{acA} + i^*_{acB} + i^*_{LdcC}\right], 0\right\} \quad (14)$$

$$f_{cC}(t) = \frac{d_C(t)}{\Delta\sigma_C} \cdot \left[S_2 \cdot \frac{V_{dc}}{L_{dcC}} - S_1 \cdot \frac{i^*_{acA}(t) + i^*_{acB}(t)}{c1C}\right] \quad (15)$$

Fig. 9 and Fig. 10 are block representations of the control system of converters C and A, respectively.

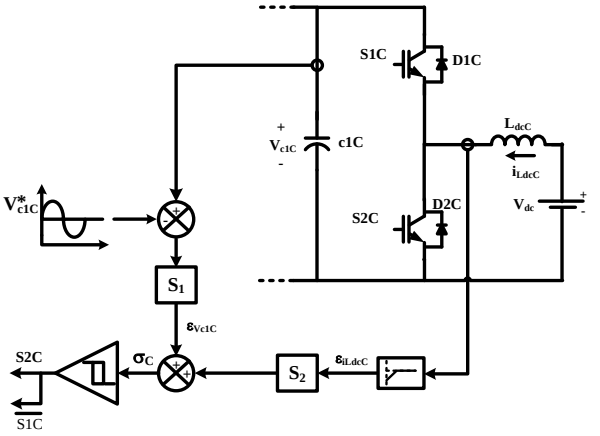

Fig. 9. Diagram of converter C with its control by sliding mode.

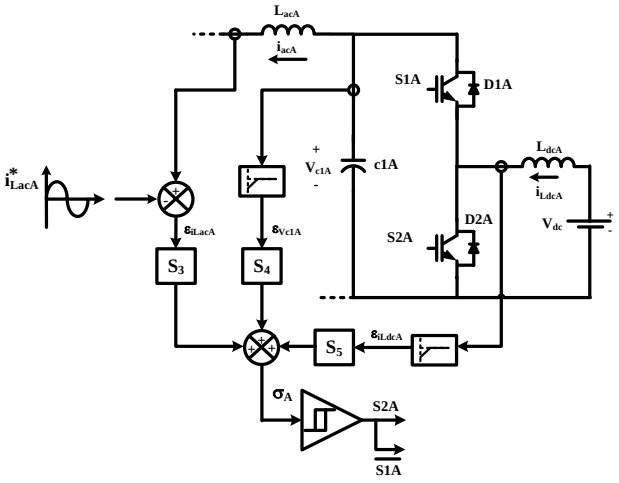

Fig. 10. Diagram of converter A with its control by sliding mode.

IV. DESIGN AND EXPERIMENTATION

In order to verify the operation of the system, a step-down three-phase prototype has been implemented, according to the scheme of Fig. 4, with the following electrical characteristics: V_{dc} = 75 V; V_{acp} = 110 V; output power P = 600 W; minimum switching frequencies: 13 kHz (converter C) and 26 kHz (converters A and B). In agreement with the established criteria, the minimum average voltage on capacitor c1C must be 185 V, according to equation (14). A more detailed approach to the design criteria can be found in [1], [2], [3], [4], and [7].

The electric parameters of converter C are; L_{dcC} =200 μH, c1C = 10 μF. The constants that describe the sliding regime surface are; S_1 = 0.029 V/V; S_2 = 0.073 V/A. The hysteresis band is defined as 0.51 V. It is used first-order high-pass filter for i_{LdcC} with a cutoff frequency of f_{pa} = 1.2 kHz.

Concerning converters A and B: $L_{acA} = L_{acB}$ = 5.1 mH are designed to filter the high-frequency switching ripple, $L_{dcA} = L_{dcB}$ = 150 μH; c1A = c1B =5 μF are polypropylene capacitors. The constants that describe the sliding regime surface are $S_3 = S_6$ = 0.322 V/A; $S_4 = S_7$ = 0.029 V/V; $S_5 = S_8$ = 1.5 Ω. The hysteresis band is 2.15 V. Four second-order Butterworth high-pass filter with cutoff frequency of f_{pa} = 1.2 kHz provide the errors corresponding to i_{LdcA} , i_{LdcB} , V_{c1A} , V_{c1B} .

Some problems, such as high-frequency radiated noise, which causes deformation in the reference signals, false drive pulses, and alteration of the error signals, did not allow to achieve rated power in the experimentation with the prototype. However, the converter is able to provide the desired current waveform in lower power levels. In this way, it is possible to verify the operation of the converter working as inverter and as rectifier in steady state.

The results obtained in the operation as inverter and as rectifier at half power ($\approx 300W$) are presented in the following figures. Initially, the curves in the operation as rectifier are presented. The voltages on the three capacitors are visualized in Fig. 11. It can be observed that the DC inductor currents (Fig. 12) present mainly 60Hz and 120Hz components, added to higher frequency components. The switching frequencies in 0°, 90°, 180° and 270° are presented in Table 1. These frequencies are lower than those defined in equation (15), due to a dead-time circuit included to allow the generation of the complementary driving pulses to the switches.

The currents in the AC inductors are shown in Fig. 13. The current and the voltage in the AC side, phase A, are shown in Fig. 14.

It can be observed that the inductor current has the 60Hz and 120 Hz components and higher frequency components. For this reason, it is possible to build these inductors with silicon-iron cores, provided that a small current ripple is allowed, so as to prevent high loss levels in the inductor cores.

By inverting the signals of reference for i_{acA} and i_{acB}, the system works as rectifier. The main results are shown in the following figures: Fig. 15 shows the voltage on the three capacitors c1A, c1B and c1C. The currents in the DC inductors are shown in Fig. 16. The currents in the AC inductors are shown in Fig. 17. The current and voltage in the AC side, phase A, are shown in Fig. 17. The switching frequencies in 0°, 90°, 180° and 270° are presented in Table 2.

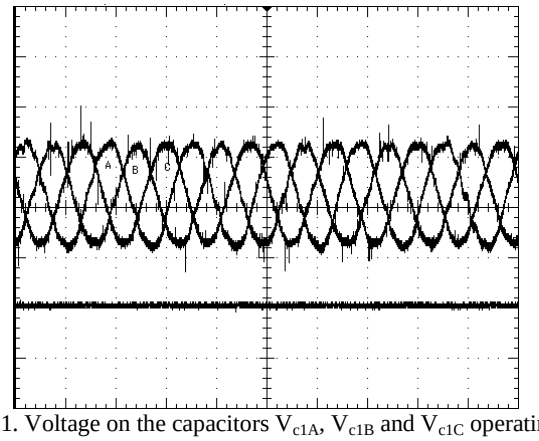

Fig. 11. Voltage on the capacitors V_{c1A}, V_{c1B} and V_{c1C} operating as inverter. (scales: 100 V/div., 10 ms/div.)

Table 1. Switching frequency for currents i_{LdcA}, i_{LdcB} and i_{LdcC} in the operation as inverter.

Frequency / Current	no load	0° (kHz)	90° (kHz)	180° (kHz)	270° (kHz)
i_{LdcA}	20,83	21,55	17,86	24,04	18,66
i_{LdcB}	21,19	19,53	15,06	25	20,49
i_{LdcC}	15,43	15,43	18,38	12,89	13,16

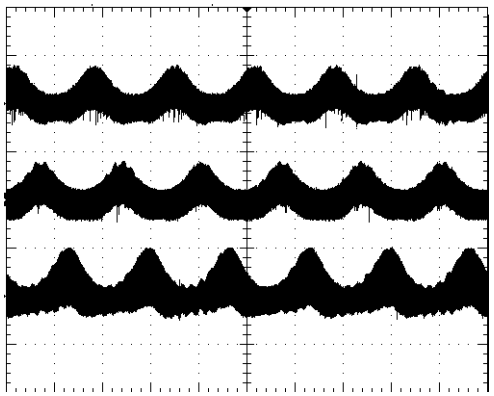

Fig. 12. Circulating currents through inductors L_{dcA}, L_{dcB} and L_{dcC} operating as inverter. (scales: 20A/div., 10 ms/div.)

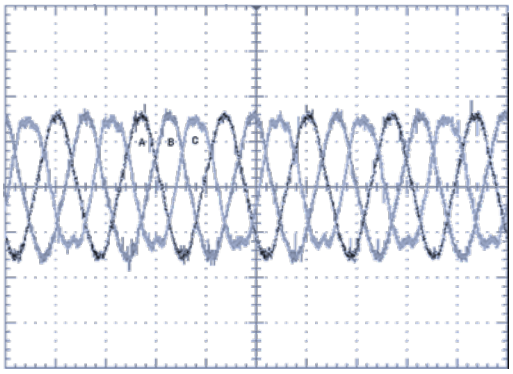

Fig. 13. Currents i_{acA}, i_{acB} and i_{acC} operating as inverter. (scales: 1A/div., 10 ms/div.)

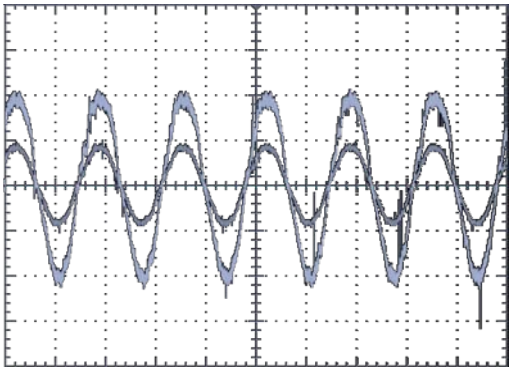

Fig. 14. Voltage (V_{acA} (t)) and current (i_{acA}) in the AC side (Phase A), operating as inverter. (scales: 50V/div., 2A/div., 10 ms/div.)

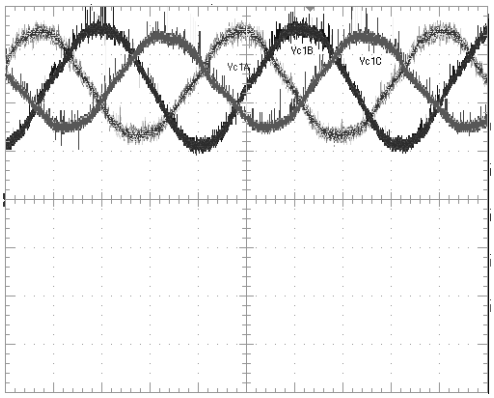

Fig. 15. Voltage on the capacitors V_{c1A}, V_{c1B} and V_{c1C} operating as rectifier. (scales: 100 V/div., 4 ms/div.)

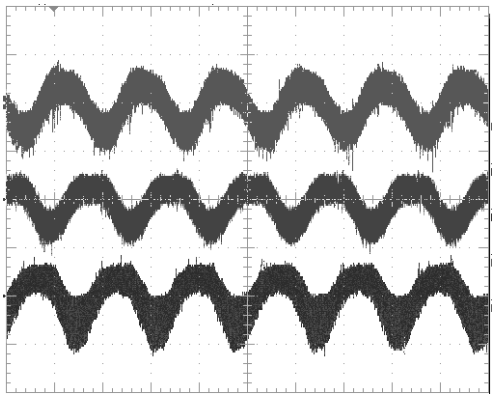

Fig. 16. Circulating currents through inductor L_{dcA}, L_{dcB} and L_{dcC} operating as rectifier. (scales: 20A/div., 10 ms/div.)

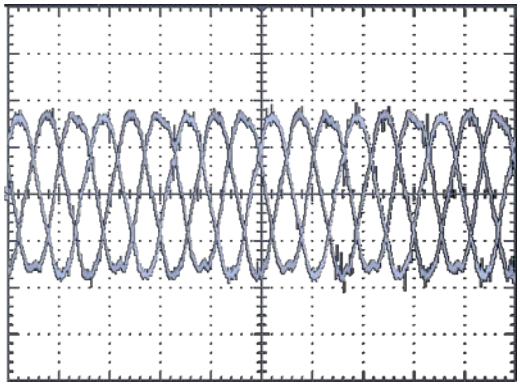

Fig. 17. Current i_{acA}, i_{acB} and i_{acC} operating as rectifier. (scales: 1A/div., 10 ms/div.)

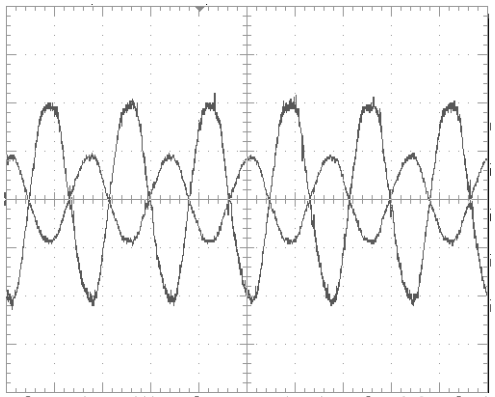

Fig. 18. Voltage ($V_{acA}(t)$) and current (i_{acA}) in the AC side (phase A), operating as rectifier. (scales: 50V/div., 2A/div., 10 ms/div.)

Table 2. Switching frequency for currents i_{LdcA}, i_{LdcB} and i_{LdcC} in the operation as rectifier.

Frequency / Current	0° (kHz)	90° (kHz)	180° (kHz)	270° (kHz)
i_{LccA}	16,39	20	21,74	20
i_{LccB}	21,74	21,28	21,74	18,52
i_{LccC}	15,15	10,64	14,29	13,7

Fig. 19 shows the total harmonic distortion of the AC currents in the operation as rectifier and as inverter. This analysis was made taking into account the first forty-nine harmonics [11].

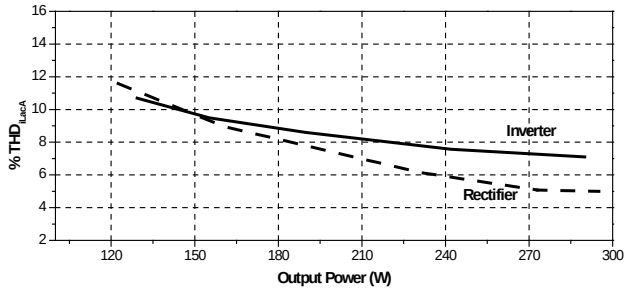

Fig. 19. Normalized current harmonics in i_{acA}, operating as rectifier and inverter.

Fig. 20 shows the power factor versus output power. As it can be seen, the converter operates with high power factor at half rated power.

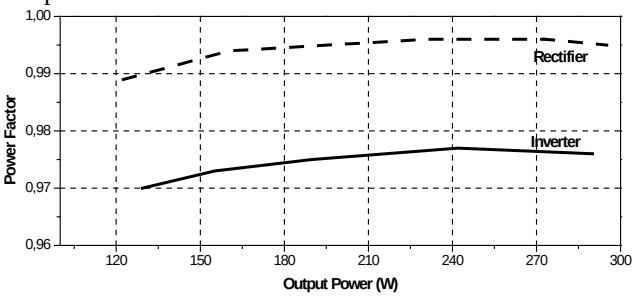

Fig. 20. Power factor versus output power in phase A, operating as rectifier and inverter.

V. CONCLUSION

The presented converter is a new contribution to the family of the three-phase rectifiers with high power factor. Some inconveniences, of course, can be listed pointed out: the switches undergo high current stress, the control technique by its nature uses hysteresis, the definition of the control parameters can become complex, the switching frequency is variable and depends on the operating point. On the other hand, its main advantages in regard to the already existing converters are:

- it is bidirectional in current;
- the output voltage can be lower, equal or greater than the peak of the input voltage;
- the converter is able to maintain the input currents, i_{acA}, i_{acB} and i_{acC} very close to the imposed sine reference (in phase with the input voltage), achieving a power factor close to unit;

It is necessary to avoid the radiated noises, since they can cause problems in the command signals. A way of avoiding problems with radiated noises could be the use of the digital control, in such a way as to generate signals of references that are not altered by external noise.

An important aspect to be highlighted is the use of high-pass filters to obtain the error signals. This technique proved to give a good approach of the error signals, but on the other hand, the control circuit loses sensitivity to the real value of the current, thus demanding additional protection schemes.

Silicon-iron cores can be used for the DC inductors, since their currents are mainly composed of DC and low-order frequencies, provided only low-ripple currents are allowed to flow through them.

The studied topology can find a large field of application, operating as inverter, in the AC power generation of energy from sources of DC voltage (photovoltaic panels, for example). In the operation as rectifier, the proposed topology offers a solution for high-power factor interconnections between the power system and loads that require DC voltage, especially in the cases where the DC levels are lower than the peak value of the available sinusoidal voltage.

VI. REFERENCES

[1] Colling, Ivan Eidt and Barbi, Ivo. “A reversible step-up voltage-source inverter controlled by sliding mode”. Charleston, South Carolina, Records of the 30th IEEE Power Electronics Specialists Conference – PESC, June-July 1999. pp. 538-543. Vol. 1.

[2] —. “Reversible Unity Power Factor Step-Up/Step-Down AC–DC Converter Controlled by Sliding Mode”. IEEE Trans. on Power Electron. No. 2, 2001, Vol. 16, pp. 223-230.

[3] Cáceres Agelviz, Ramón O. and Barbi, Ivo. "A Boost DC-AC converter: operation, analysis, control and experimentation". International Conf. on Ind. Electron., Control, and Instrumentation – IECON, Orlando, USA, 1995. v.1,p.546-551.

[4] —. "A boost DC-AC converter: operation, analysis, control and experimentation". New York : IEEE Trans. on Power Electron., 1999. pp. 134-141. Vol. 14.

[5] Carpita, M. and Marchesoni, M. “Experimental study of a Power conditioning using sliding mode control”. IEEE Trans. Power Electron. Sept. 1996, Vol. 11, pp. 731-742.

[6] Colling, Ivan Eidt and Barbi, Ivo. “Conversor CA-CC trifásico reversível com elevado fator de potência e controle por regime de deslizamento” (A reversible three-phase AC-DC converter with high power factor controlled by sliding regime), XIII Congresso Brasileiro de Automática - CBA. Florianópolis, Brazil, Sept. 2000. pp. 711-716.

[7] Vidal, Edward Fuentealba, Colling, Ivan Eidt and Barbi, Ivo. “AC-DC Three-Phase Reversible Converter With High Power Factor Controlled By Sliding Regime”. Brazilian Power Electronics Conference – COBEP, Blumenau, Brazil, Sept. 2007.

[8] DeCarlo, Raymond, Zak, Stanislaw and Matthews, Gregory P. “Variable Structure Control of Nolinear Multivariable System”. New York : Tutorial Proc. of the IEEE, 1988. pp. 212-232. Vol. 76.

[9] Utkin, V. I. “Variable structure systems with sliding modes”. IEEE Trans. on Automatic Control. April 1997, Vol. 22, No. 2, pp. 212-222.

[10] Venkataramanan, Ram, Savanovic, Adif and Cuk, Slobodan. "Sliding mode controle f DC-to-DC converters". International Conf. on Ind. Electron., Control and Instrumentation - IECON. 1985.

[11] International Electrotechnical Commission. "Electromagnetic compatibility (EMC) Part1-2:limits - Limits for harmonic current emissions (equipament input current 16 A per phase), IEC 61000 3-2", 2nd Edition, 2000.

[12] Cáceres Agelviz, Ramón Oswaldo. “Família de Conversores CC-CA, Derivados dos Conversores CC-CC Fundamentais”. (A Family of DC-AC Converters, Derived from the Fundamental DC-DC Converters). Doctoral Thesis on Electrical Engineering, Institute of Power Electronics, Federal University of Santa Catarina, Florianópolis, Brazil, 1997.

[13] Colling Ivan Eidt. “Conversores CA-CC monofásicos e Trifásicos reversíveis com elevado fator de potência”. (Reversible Single-Phase and Three-Phase AC-DC Converters with High Power Factor). Doctoral Thesis on Electrical Engineering, Institute of Power Electronics, Federal University of Santa Catarina, Florianópolis, Brazil, 2000.

[14] Vidal, Edward Fuentealba. “Retificadores Bidirecionais Monofásicos e Trifásicos com Carga Diferencial Controlados por Regime de Deslizamento”. (Single-Phase and Three-Phase Bidirectional Rectifiers with Differential Load and Controlled by Sliding Regime). Doctoral Thesis on Electrical Engineering. 2008 , Institute of Power Electronics, Federal University of Santa Catarina, Florianópolis, Brazil, 2008.